Scalable recovery of missing blocks in time series with high and low cross-correlations

Khayati, Mourad ; Cudré-Mauroux, Philippe ; Böhlen, Michael Hanspeter

Abstract: Missing values are very common in real-world data including time-series data. Failures in power, communication or storage can leave occasional blocks of data missing in multiple series, affecting not only real-time monitoring but also compromising the quality of data analysis. Traditional recovery (imputation) techniques often leverage the correlation across time series to recover missing blocks in multiple series. These recovery techniques, however, assume high correlation and fall short in recovering missing blocks when the series exhibit variations in correlation. In this paper, we introduce a novel approach called CDRec to recover large missing blocks in time series with high and low correlations. CDRec relies on the centroid decomposition (CD) technique to recover multiple time series at a time. We also propose and analyze a new algorithm called Incremental Scalable Sign Vector to efficiently compute CD in long time series. We empirically evaluate the accuracy and the efficiency of our recovery technique on several real-world datasets that represent a broad range of applications. The results show that our recovery is orders of magnitude faster than the most accurate algorithm while producing superior results in terms of recovery.

DOI: https://doi.org/10.1007/s10115-019-01421-7

Knowledge and Information Systems manuscript No.
(will be inserted by the editor)

Scalable Recovery of Missing Blocks in Time Series with High and Low cross-Correlations

Mourad Khayati · Philippe Cudré-Mauroux · Michael H. Böhlen

Received: date / Accepted: date

Abstract Missing values are very common in real-world data including time series (sensor) data. Failures in power, communication or storage can leave occasional blocks of data missing in multiple series, affecting not only real-time monitoring but also compromising the quality of data analysis. Traditional recovery (imputation) techniques often leverage the correlation across time series to recover these missing blocks. However, these techniques assume highly correlated time series and fall short in recovering missing blocks when the series exhibit variations in correlation (high and low).

In this paper, we introduce a novel approach called CDRec to recover large missing blocks in time series with variations in correlation. CDRec relies on the Centroid Decomposition (CD) technique to recover multiple time series at a time. We also propose and analyze a new algorithm called Incremental Scalable Sign Vector (ISSV) that efficiently compute CD in long time series. We empirically evaluate the accuracy and the efficiency of our recovery technique on several real-world datasets that represent a broad range of applications. The results show that our recovery is orders of magnitude faster than the most accurate algorithm while producing superior results in terms of recovery.

Keywords Recovery of missing blocks · Centroid Decomposition · time series · Correlation.

This project has received funding from the European Union's Horizon 2020 research and innovation programme under grant agreement No 732328.

Mourad Khayati, Philippe Cudré-Mauroux
eXascale Infolab, University of Fribourg, Switzerland
E-mail: {firstname.lastname}@unifr.ch

Michael H. Böhlen
Department of Informatics, University of Zurich, Switzerland

1 Introduction

Time series data can be found in nearly every domain, for example, climate, traffic, finance, energy industry and medicine. But nearly everywhere, where data is measured and recorded, missing values occur (e.g, the Intel Berkeley research lab dataset [7] is missing about 50%, the UCI repository of time series [11] is missing about 20%). Missing values often appear consecutively, forming a block in a time series. Some missing blocks can be rather large, because, for instance, it can take minutes, hours or even days for a broken sensor to be replaced. Data management systems assume no such gaps exist in the data. Even if a system can work with incomplete data (e.g., NULLs in relational databases), leaving missing values untreated can cause incorrect or ill-defined results [8].

The recovery of missing values is a well studied area, where lots of research has been already done. Several techniques have been proposed to recover missing values, but only a few of them are able to handle large missing blocks (see Section 2). Existing block-recovery algorithms often leverage the correlation across time series. These techniques, however, fall short when time series exhibiting variations in correlation are used. This limits the recovery accuracy since using both highly and lowly correlated time series can be beneficial for the recovery process [17].

In this paper, we study the problem of the recovery of missing blocks in multiple univariate time series[1] exhibiting variations in correlation. More specifically, we introduce a new matrix-based algorithm called CDRec that accurately recovers missing blocks in highly and lowly correlated time series. Unlike standard matrix completion techniques [24,26], our technique embeds the time series' cross-correlation into its optimization problem and thus, makes it possible to take into account the variation in correlation.

At the technical level, our recovery technique relies on the Centroid Decomposition (CD) technique. The latter decomposes an $n \times m$ input matrix $\mathbf{X}$ into the product of two matrices, $\mathbf{X} = \mathbf{L} \cdot \mathbf{R}^T$, where $\mathbf{L}$ and $\mathbf{R}$ are called the *loading* and *relevance* matrix, respectively, and $\mathbf{R}^T$ denotes the transpose of $\mathbf{R}$. Each loading and relevance column (vector) is determined based on a maximal centroid value, $\max \|\mathbf{X}^T \cdot Z\|$, which is equal to the norm of the product between the transpose of the input matrix and a sign vector Z consisting of 1s and -1s. Finding the *maximizing sign vector* that maximizes the centroid value is at the core of the CD method. The most efficient algorithm to compute the maximizing sign vector [9] requires the construction of a correlation matrix with a quadratic space complexity. This complexity hinders the application of CD to recover long time series.

To solve the scalability problem of CD, we introduce a new algorithm called Incremental Scalable Sign Vector *(ISSV)* that efficiently computes the maximizing sign vector for an $n \times m$ input matrix, $\mathbf{X}$, that represents m time series with n observations each. Compared to the technique introduced in [9], the proposed solution does not require the construction of a correlation matrix, thus reduces the space. Compared to our earlier technique introduced in [18], the proposed solution computes the weight vectors in an incremental fashion, thus speeds up the computation.

[1] We consider time series with equally spaced granularity.

In summary, the main contributions of this paper are as follows:

- We introduce a new parameter-free algorithm based on the Centroid decomposition technique to recover large missing blocks in multiple time series. Our algorithm is able to handle time series with high variations in correlation.
- We propose a new sign vector computation algorithm, called Incremental Scalable Sign Vector (ISSV), that reduces the space complexity of the Centroid Decomposition technique from quadratic to linear and improves by one order of magnitude the runtime complexity compared to the state-of-the-art solution.
- We present the results of an experimental evaluation of the recovery accuracy and efficiency of CDRec, and the efficiency and the correctness of ISSV on real-world time series. The results show that CDRec is orders of magnitude faster than the most accurate algorithm while producing superior results in terms of recovery.

The remainder of this paper is organized as follows. Section 2 discusses related work. Section 3 provides preliminary concepts and definitions. Section 4 describes the CDRec algorithm that uses the Centroid Decomposition to recover missing blocks in time series. Section 5 introduces the ISSV algorithm to compute the sign vector used by CD in linear space complexity and discusses its properties. Section 6 reports the results of our experiments. Section 7 concludes the paper and points to future work.

2 Related Work

2.1 Centroid Decomposition

The Centroid Decomposition is a matrix decomposition technique that computes the loading and the relevance vectors out of an input matrix $\mathbf{X}$. The most challenging part of CD is the computation of the sign vector Z, consisting of 1s and -1s, that maximizes $\|\mathbf{X}^T \cdot Z\|$, where $\mathbf{X}^T$ is the transpose of $\mathbf{X}$ and $\|\cdot\|$ denotes the norm of a vector. The classical approach is based on the centroid method [10] with a brute force search through an exponential number of sign vectors (see Section 3.3). This yields an exponential time and linear space complexity. Chu et al. [9] introduce a more efficient algorithm to find the maximizing sign vector, which we refer to as *Quadratic Sign Vector* (QSV). The authors consider the set of all possible sign vectors as an n-dimensional hypercube, where each node represents a sign vector and is connected with all nodes representing a sign vector that differs in exactly one element. The QSV algorithm performs the search through a traversal along the nodes of the hypercube. QSV achieves a quadratic runtime complexity and its space complexity is quadratic too because of the construction of the correlation matrix. In [18] we introduce the SSV algorithm that computes the sign vectors without the construction of the covariance/correlation matrix and achieves a linear space complexity. The main idea of SSV is as follows: instead of searching for the maximizing sign vector using all elements of the input matrix $\mathbf{X}$, SSV searches for it by rows of $\mathbf{X}$. The search is performed by iteratively computing a weight vector V, derived from $\mathbf{X}$, which is then used to select

the element in Z that needs to be flipped. The weight vector is obtained through mapping the original optimization problem that CD solves onto a different and equivalent optimization problem.

This work extends our earlier results [18] as follows. First, we introduce the CDRec algorithm that uses CD to recover missing blocks in time series and describe its properties (cf. Section 4). Second, we introduce the ISSV technique to incrementally compute the sign vectors, yielding a faster CD computation compared to the SSV technique (cf. Section 5). Next, we prove that, among all possible sign flipping strategies, our strategy is the only one that reaches the global optimum (cf. Section 5.3). Finally, we empirically compare the recovery accuracy of CDRec against the state-of-the-art recovery techniques we describe hereafter (cf. Section 6).

2.2 Large Missing-Block Recovery Techniques

Several statistical techniques have been proposed in the literature to recover missing values such as Regression [13], MeanImpute [14], kNNImpute [34], etc. Data analysis tools, such as R package, implement a wide range of these statistical techniques[2]. These techniques are, however, effective only in the case of single or a handful of missing values and are not suitable in the case of large missing blocks [23, 35], which is the main focus of this paper. In what follows we describe three different categories of techniques designed to recover missing blocks in time series data.

Matrix-based techniques. They recover missing blocks by looking at an entire set of series as a matrix and by applying techniques based on matrix completion principles. These algorithms rely on different matrix decomposition/factorization techniques such as Principal Components Analysis, Matrix Factorization, Non-Negative Matrix Factorization and Singular Spectrum Analysis.

In [33], the authors propose the TRMF technique that uses Matrix Factorization (MF) to recover missing blocks in multidimensional time series. MF takes an $n \times m$ input matrix $\mathbf{X}$ and approximates it using two factor matrices, $\mathbf{W}$ and $\mathbf{H}$ respectively of size $n \times r$ and $r \times m$ such that $\mathbf{X} \approx \mathbf{W} \cdot \mathbf{H}$. The resulting factoriztation is embedded with a new temporal autoregressive regularizer to learn the dependencies across the input time series. The temporal dependencies are then used to infer replacement values for the missing ones. TRMF resorts to an autoregressve model, which makes it not scalable for large time series.

Mei et al. [20] propose a temporal NonNegative matrix Factorization (NMF)-based technique called TeNMF to recover missing blocks. NMF is similar to the above MF technique, but it constrains $\mathbf{W}$ and $\mathbf{H}$ to contain non-negative elements only. The authors formalize the matrix recovery problem as a minimization of a quadratic nonnegative loss function of the difference between $\mathbf{V}$ and the product $\mathbf{W} \cdot \mathbf{H}$. Then, a penalization term is introduced into the loss function to take into account for the cross-correlation between time series. TeNMF's recovery is sensitive to negative correlations as it resorts to NMF principles.

[2] `https://cran.r-project.org/web/views/MissingData.html`

Balzano et al. [5,6] propose a Principal Component Analysis (PCA)-based recovery technique called GROUSE. PCA takes an $n \times m$ input matrix $\mathbf{X}$ and finds n components each of size m that approximate the dimensions of the initial data. Grouse applies an incremental gradient descent procedure on a defined cost function to track the co-evolving dimensions and subsequently derive the missing values. The proposed technique does not initialize the missing values rendering GROUSE's recovery unstable.

In [2,3], the authors introduce a recovery algorithm that relies on the Singular Spectrum Analysis (SSA) technique. The proposed technique takes the input time series and constructs a so called page matrix (a non overlapping Hankel matrix[3]). Then, the Singular Value Decomposition (SVD) [22] is applied to the Page matrix in order to extract the singular values. The latter are grouped depending on the model that generates the time series and used to approximate the original matrix. The approximated matrix is used as a source of replacement for the missing values. This technique does not support multiple incomplete time series.

Pattern-based Techniques. These techniques consider that sensors which are at close proximity can present trend similarity. They apply pattern matching techniques and use the observed values, the values that the sensors actually measured, as a source of replacement.

TKCM [30] is a continuous technique to recover missing blocks in correlated time series streams. It first defines a pattern as interval of points, across all time series, that contains the missing value. Then, it searches for the k most similar non-overlapping patterns to the defined pattern and returns the average of points over the k patterns as an estimation of the missing value. TKCM is able to handle linear and non-linear correlated time series and performs a scalable recovery that is linear with the length of time series. TKCM is designed for time series with repeating trends and is not capable of recovering multiple time series at a time.

Yi et al. [31] introduce the STMVL technique to recover missing blocks in geosensory time series. The proposed technique leverages the temporal (closeness of the values in time) and spatial (distance between time series) correlation between time series. STMVL combines a user-based and item-based collaborative filtering with statistical smoothing models to derive models out of the historical data. The missing values are then estimated using the generated models and the spatio-temporal coordinates of values. STMVL assumes the input time series to be highly correlated.

Network-based techniques. These algorithms build a (parametric) model which reconstructs the linear dependence between time series. The recovery is based on information obtained through those dependencies.

Yoon et al. [32] introduce a Neural Network (NN)-based solution called MRNN to recover missing blocks. The proposed solution first initializes the missing values using linear interpolation and then applies a multi-directional Recurrent network to recover the missing data. MRNN learns the data dependencies by leveraging both the correlation within time series and the correlation across time series. MRNN was designed for medical data where time series are dependent on one another.

[3] https://en.wikipedia.org/wiki/Hankel_matrix

In [19], the authors introduce a Deep Network-based recovery technique called DeepIN. The proposed technique is designed for a smart city environment where the missing blocks follow a repeating pattern. DeepIN uses multiple LSTM (Long Short Term Memory) models to learn the temporal-spatial dependencies across time series and assumes the time series to be highly correlated.

In Section 6, we compare the efficiency and accuracy of CDRec against all the aforementioned recovery, except DeepIN, for which no source code is publicly available. Our results show that, in addition to be parameter-free, our recovery outperforms the state of the art.

3 Background

3.1 Notations and Definitions

Bold upper-case letters refer to matrices, regular font upper-case letters refer to vectors (rows and columns of matrices) and lower-case letters to refer to elements of vectors/matrices. For example, $\mathbf{X}$ is matrix, X_{i*} is the i-th row of $\mathbf{X}$, X_{*i} is the i-th column of $\mathbf{X}$, $(X_{i*})^T$ is the transpose of X_{i*} and x_{ij} is the j-th element of X_{i*}. The isolated column vectors that do not belong to a matrix will be denoted with a capital letter, e.g., V.

A *time series* $X = \{(t_1, v_1), \ldots, (t_n, v_n)\}$ is an ordered set of n temporal values v_i that are ordered according to their timestamps t_i. In the rest of the paper we omit the timestamps, since they are ordered, and write the time series $X_1 = \{(0,2),(1,0),(2,\text{-}4)\}$ as the ordered set $X_1 = \{2,0,\text{-}4\}$. We write $\mathbf{X} = [X_{*1}|\ldots|X_{*m}]$ (or $\mathbf{X}_{n\times m}$) to denote an $n \times m$ matrix having m time series X_{*j} as columns and n values for each time series as rows.

A *sign vector* $Z \in \{1,\text{-}1\}^n$ is a sequence $[z_1, \ldots, z_n]$ of n unary elements, i.e., $|z_i| = 1$ for $i = \{1, \ldots, n\}$.

We use the symbol $\times$ for scalar multiplications and the symbol $\cdot$ for matrix multiplications. The symbol $\|\|$ refers to the l-2 norm of a vector. Assume $X = [x_1, \ldots, x_n]$, then $\|X\| = \sqrt{\sum_{i=1}^{n}(x_i)^2}$.

3.2 Centroid Decomposition

The *Centroid Decomposition (CD)* decomposes an $n \times m$ matrix, $\mathbf{X} = [X_{*1}|\ldots|X_{*m}]$, into an $n \times m$ loading matrix, $\mathbf{L} = [L_{*1}|\ldots|L_{*m}]$, and an $m \times m$ relevance matrix, $\mathbf{R} = [R_{*1}|\ldots|R_{*m}]$, i.e.,

$$\mathbf{X} = \mathbf{L} \cdot \mathbf{R}^T = \sum_{i=1}^{m} L_{*i} \cdot (R_{*i})^T$$

where $\mathbf{R}^T$ denotes the transpose of $\mathbf{R}$.

The function CD describes the Centroid Decomposition procedure of an $n \times m$ input matrix $\mathbf{X}$. At each iteration i, the *maximizing sign vector* Z (described in Section 3.3) is computed, and used to subsequently compute the i-th relevance and loading vectors. Next, a matrix reduction step is applied in order to obtain the next relevance and loading vectors. The algorithm terminates when m loading and relevance vectors, of size n and m respectively, are computed. Note that the m maximizing sign vectors are different and independent from each other.

function CD($\mathbf{X}$, n, m)
  $i := 1$
  repeat
    $Z_i := FindMaxSV(\mathbf{X}, n, m)$
    $C_i := \|\mathbf{X}^T \cdot Z_i\|$
    $R_i := \frac{C_i}{\|C_i\|}$
    $L_i := \mathbf{X} \cdot R_i$
    $\mathbf{X} := \mathbf{X} - L_i \cdot R_i^T$
    $i := i + 1$
  until $i = m$;
  return $\mathbf{L}, \mathbf{R}$
end function

Example 1 (Centroid Decomposition) *To illustrate the computation of CD, consider the input matrix,* $\mathbf{X}$*, that contains three time series of five elements each as a running example, i.e.,*

$$\mathbf{X} = \begin{bmatrix} 6 & 3 & 3 \\ -2 & 2 & 2 \\ -7 & 1 & -5 \\ -3 & 4 & -1 \\ 2 & -4 & 2 \end{bmatrix}$$

Among all sign vectors, the sign vector that maximizes $\|\mathbf{X}^T \cdot Z\|$ *is* $Z_1 = \{-1, 1, 1, 1, -1\}^T$ *(see Section 3.3).* Z_1 *is used to compute the first column of* $\mathbf{R}$ *(and* $\mathbf{L}$*) during iteration 1 as follows:*

$$R_{*1} = \frac{\mathbf{X}^T \cdot Z_1}{\|\mathbf{X}^T \cdot Z_1\|} = \begin{bmatrix} 0.86 \\ 0.19 \\ 0.48 \end{bmatrix}; \quad L_{*1} = \mathbf{X} \cdot R_{*1} = \begin{bmatrix} 5.27 \\ -1.63 \\ -8.27 \\ -4.33 \\ 3.86 \end{bmatrix}$$

Similarly, the second and third columns of $\mathbf{R}$ *(and* $\mathbf{L}$*) are computed using the second and third maximizing sign vectors (derived from* $\mathbf{X} - L_{*1} \cdot R_{*1}^T$*) respectively. The resulting decomposition produced by CD is (only two decimals are shown):*

$$\mathbf{X} = \begin{bmatrix} 6 & 3 & 3 \\ -2 & 2 & 2 \\ -7 & 1 & -5 \\ -3 & 4 & -1 \\ 2 & -4 & 2 \end{bmatrix} = \underbrace{\begin{bmatrix} 5.27 & 5 & 1.1 \\ -1.63 & 2.19 & -2.14 \\ -8.27 & -2.33 & 1.1 \\ -4.33 & 2.67 & 0.41 \\ 3.86 & -2.48 & -1.73 \end{bmatrix}}_{\mathbf{L}} \cdot \underbrace{\begin{bmatrix} 0.86 & -0.34 & 0.39 \\ 0.19 & 0.91 & 0.38 \\ 0.48 & 0.25 & -0.84 \end{bmatrix}}_{\mathbf{R}^T}$$

3.3 Maximizing Sign Vector

Given an $n \times m$ matrix $\mathbf{X}$, the *maximizing* sign vector Z maximizes the *centroid value* $\|\mathbf{X}^T \cdot Z\|$, i.e., Z satisfies the following equation:

$$\underset{Z \in \{1,-1\}^n}{\arg\max} \|\mathbf{X}^T \cdot Z\|. \tag{1}$$

To illustrate the computation of the maximizing sign vector, consider the same input matrix from our running example. We proceed by enumerating all possible sign vectors and we compute $\|\mathbf{X}^T \cdot Z\|$ for each of them (the computed values are displayed below the sign vectors).

$$\begin{array}{ccccccccccc}
Z_1 & Z_2 & Z_3 & Z_4 & Z_5 & Z_6 & Z_7 & & Z_{10} & & Z_{32} \\
\begin{bmatrix} 1 \\ 1 \\ 1 \\ 1 \\ 1 \end{bmatrix} & \begin{bmatrix} -1 \\ 1 \\ 1 \\ 1 \\ 1 \end{bmatrix} & \begin{bmatrix} 1 \\ -1 \\ 1 \\ 1 \\ 1 \end{bmatrix} & \begin{bmatrix} 1 \\ 1 \\ -1 \\ 1 \\ 1 \end{bmatrix} & \begin{bmatrix} 1 \\ 1 \\ 1 \\ -1 \\ 1 \end{bmatrix} & \begin{bmatrix} 1 \\ 1 \\ 1 \\ 1 \\ -1 \end{bmatrix} & \begin{bmatrix} -1 \\ -1 \\ 1 \\ 1 \\ 1 \end{bmatrix} & \cdots & \begin{bmatrix} -1 \\ 1 \\ 1 \\ 1 \\ -1 \end{bmatrix} & \cdots & \begin{bmatrix} -1 \\ -1 \\ -1 \\ -1 \\ -1 \end{bmatrix} \\
7.2 & 16.7 & 3.6 & 15.3 & 4.1 & 16.4 & 15.5 & & 23.3 & & 7.2
\end{array}$$

Among all sign vectors, Z_{10} and its sign opposite give the same and maximum centroid value $\|\mathbf{X}^T \cdot Z\| = 23.3$, and is thus the maximizing sign vector. Assume that $diag^{=0}(\mathbf{X})$ is an auxiliary function that sets the diagonal values of an $n \times n$ matrix to 0, then according to Lemma 1 in [18], the following equivalence holds:

$$\underset{Z \in \{1,-1\}^n}{\arg\max} \|\mathbf{X}^T \cdot Z\| \equiv \underset{Z \in \{1,-1\}^n}{\arg\max} Z^T \cdot V \tag{2}$$

where $V = diag^{=0}(\mathbf{X} \cdot \mathbf{X}^T) \cdot Z$. The elements of V are defined as follows:

$$v_i = z_i(z_i \times X_{i*} \cdot S - (X_{i*} \cdot (X_{i*})^T)) \tag{3}$$

where v_i is the i-th element of the weight vector V and $S = \sum_{i=1}^{n} (z_i \times (X_{i*})^T)$.

In the next section, we describe the CDRec algorithm that uses CD to recover missing blocks in time series.

4 Recovery of Missing Blocks

In this section, we first describe the CDRec technique that uses the Centroid Decomposition technique to recover missing blocks in time series. Then, we describe the properties of the recovery.

4.1 Recovery process

Algorithm 1 uses CD to recover missing blocks in multiple time series at a time. It takes as input a matrix $\mathbf{X}$ that contains a set of missing blocks $\mathbf{X}_B$ and a list T^- of pairs indicating the rows and columns of the missing values in $\mathbf{X}$. We normalize the data using the z-score normalization technique [16]. The recovery starts by initializing $\mathbf{X}_B$ using either linear interpolation or extrapolation, depending on the position of the missing block(s) in $\mathbf{X}$ (line 2). Then, we apply a truncation to the decomposition of $\mathbf{X}$ to return $\mathbf{L}_k$ and $\mathbf{R}_k$ which contain the first k columns of $\mathbf{L}$ and $\mathbf{R}$ respectively (line 6). To dynamically set, at each iteration, the truncation factor k, we utilize the commonly used entropy method (described later). Next, the values in $\mathbf{X}$ with positions in T^- are updated with their corresponding ones in $\mathbf{X}_k = \mathbf{L}_k \cdot \mathbf{R}_k^T$ (lines 8-9). On line 10, we cache the computed sign vector and we use it as an initial sign vector in the CD computation of the next iteration of the recovery. The recovery process terminates if the relative difference in Frobenius norm $\|\mathbf{X}_B - \widetilde{\mathbf{X}}_B\|_F/|B| = \sqrt{\sum_{i=1}^{|B|}(\tilde{x}_i - \tilde{x}_i')^2}/|B|$ between $\widetilde{\mathbf{X}}_B$ and $\mathbf{X}_B$ (where $\tilde{x}_i \in \mathbf{X}$, $\tilde{x}_i \in \widetilde{\mathbf{X}}$ and $|B|$ is the length of the missing block) falls below a small threshold value ε (by default 10^{-5}).

Algorithm 1: CDRec($\mathbf{X}$, T^-)

Input : $n \times m$ matrix $\mathbf{X}$; List of missing time points T^-
Output: Matrix with recovered values $\widetilde{\mathbf{X}}$

1 Linearly interpolate/extrapolate all missing values in $\mathbf{X}$;
2 $Z_{init} \coloneqq [1, \ldots, 1]$;
3 **repeat**
4 $\quad \widetilde{\mathbf{X}} \coloneqq \mathbf{X}$;
5 $\quad$ compute truncation factor k of $\mathbf{X}$; ▷ `using Entropy-based technique`
6 $\quad [\mathbf{L}_k, \mathbf{R}_k, Z] \coloneqq CD(\mathbf{X}, n, k, Z_{init})$;
7 $\quad \mathbf{X}_k \coloneqq \mathbf{L}_k \cdot (\mathbf{R}_k)^T$;
$\quad$ `// Update missing values`
8 $\quad$ **foreach** $(i, j) \in T^-$ **do**
9 $\quad\quad \tilde{x}_{ij} \coloneqq y_{ij}$;
$\quad\quad$ `//` y_{ij} `element of` $\mathbf{X}_k$ `at timestamp` i
10 $\quad Z_{init} \coloneqq Z$; ▷ `cache the sign vector`
11 **until** $\frac{\|\mathbf{X}_B - \widetilde{\mathbf{X}}_B\|_F}{|B|} < 10^{-5}$;
12 **return** $\widetilde{\mathbf{X}}$;

Example 2 *Let's take the example of the input matrix* $\mathbf{X}$ *from our running example (cf. Example 1). We illustrate the application of CDRec to recover a missing block (in gray) in the first time series.*

$$\underbrace{\begin{bmatrix} 6 & 3 & 3 \\ -2 & 2 & 2 \\ -7 & 1 & -5 \\ -3 & 4 & -1 \\ 2 & -4 & 2 \end{bmatrix}}_{\mathbf{X}} \rightarrow \underbrace{\begin{bmatrix} 6 & 3 & 3 \\ -2 & 2 & 2 \\ - & 1 & -5 \\ - & 4 & -1 \\ 2 & -4 & 2 \end{bmatrix}}_{\mathbf{X}_{miss}} \rightarrow \underbrace{\begin{bmatrix} 6 & 3 & 3 \\ -2 & 2 & 2 \\ -0.66 & 1 & -5 \\ 0.66 & 4 & -1 \\ 2 & -4 & 2 \end{bmatrix}}_{\mathbf{X}_{init}} \rightarrow \underbrace{\begin{bmatrix} 6 & 3 & 3 \\ -2 & 2 & 2 \\ -5.1 & 1 & -5 \\ -1.06 & 4 & -1 \\ 2 & -4 & 2 \end{bmatrix}}_{\widetilde{\mathbf{X}}_1} \rightarrow \cdots \rightarrow \underbrace{\begin{bmatrix} 6 & 3 & 3 \\ -2 & 2 & 2 \\ -6.98 & 1 & -5 \\ -4 & 4 & -1 \\ 2 & -4 & 2 \end{bmatrix}}_{\widetilde{\mathbf{X}}_p}$$

First, the missing block in $\mathbf{X}_{miss}$ is initialized and the resulting matrix, $\mathbf{X}_{init}$, is decomposed using a truncation factor $k = 1$ to produce $\mathbf{L}_1$ and $\mathbf{R}_1^T$. By multiplying $\mathbf{L}_1$ and $\mathbf{R}_1^T$ we obtain $\widetilde{\mathbf{X}}_1$. After applying the same process p times, the final $\widetilde{\mathbf{X}}_p$ containing the recovered values is obtained. Using longer time series helps to improve the accuracy of the recovery as described in Section 6.

To dynamically set the truncation factor k, we use an entropy-based method. Let $\mathbf{X}$ be an input matrix of n rows and m columns with $n \gg m$ and let $f_k = \frac{\|\mathbf{X}^T \cdot Z_k\|}{\sum_{i=1}^{m}(\|\mathbf{X}^T \cdot Z_k\|)^2}$ be the relative contribution of the k-th centroid value to the Frobenius norm. Then, the entropy of the centroid values is defined as follows:

$$E = -\frac{1}{\log m}\sum_{i=1}^{m} f_i \log f_i \tag{4}$$

The entropy E is used to find the appropriate truncation factor for the recovery process. More specifically, at each iteration of Algorithm 1, we select the smallest k such that $\sum_{i=1}^{k} f_i \geq E$. Since the entropy (used to find the truncation value k) minimizes the Frobenius norm [4] as does the iterative process, then our recovery quickly converges (cf. Section 6.2.3).

4.2 Recovery Properties

The following lemma shows that the recovery of the CDRec algorithm embeds the correlation across the input time series.

Lemma 1 *Let $\mathbf{X}$ be an $n \times m$ input matrix containing m time series where some of them have missing blocks. Then, the recovery of CDRec is based on the summation of the correlation between time series.*

Proof 1 *From* (2) *we have*

$$V = diag^{=0}(\mathbf{X}\cdot\mathbf{X}^T)\cdot Z = diag^{=0}(\begin{bmatrix} x_{11}\ldots x_{1n} \\ x_{21}\ldots x_{2n} \\ \vdots \\ x_{m1}\ldots x_{mn} \end{bmatrix} \cdot \begin{bmatrix} x_{11} & x_{21}\ldots x_{m1} \\ & \vdots \\ x_{1n} & x_{2n}\ldots x_{mn} \end{bmatrix})\cdot Z$$

Let $\bar{x}_{*i}$ and σ_{*i} be respectively the mean and the standard deviation of X_{*i}. Since each column of $\mathbf{X}$ is z-score normalized, it follows

$$V = diag^{=0}(\begin{bmatrix} \frac{x_{11}-\bar{x}_{*1}}{\sigma_{*1}} \cdots \frac{x_{1n}-\bar{x}_{*n}}{\sigma_{*n}} \\ \frac{x_{21}-\bar{x}_{*1}}{\sigma_{*1}} \cdots \frac{x_{2n}-\bar{x}_{*n}}{\sigma_{*n}} \\ \vdots \\ \frac{x_{21}-\bar{x}_{*1}}{\sigma_{*1}} \cdots \frac{x_{2n}-\bar{x}_{*n}}{\sigma_{*n}} \end{bmatrix} \cdot \begin{bmatrix} \frac{x_{11}-x_{*1}}{\sigma_{*1}} & \frac{x_{21}-x_{*1}}{\sigma_{*1}} \cdots \frac{x_{21}-x_{*1}}{\sigma_{*1}} \\ & \vdots \\ \frac{x_{1n}-x_{*n}}{\sigma_{*n}} & \frac{x_{2n}-x_{*n}}{\sigma_{*n}} \cdots \frac{x_{2n}-x_{*n}}{\sigma_{*n}} \end{bmatrix})\cdot Z \tag{5}$$

Consider the product of the first row of $\mathbf{X}$ *and the the first column of* $\mathbf{X}^T$*. we have*

$$\left[\frac{x_{11}-\bar{x}_{*1}}{\sigma_{*1}} \cdots \frac{x_{1n}-\bar{x}_{*n}}{\sigma_{*n}}\right] \cdot \begin{bmatrix} \frac{x_{11}-\bar{x}_{*1}}{\sigma_{*1}} \\ \vdots \\ \frac{x_{1n}-\bar{x}_{*n}}{\sigma_{*n}} \end{bmatrix} = \frac{\sum_{i=1}^{n}(x_{1i}-\bar{x}_{*i})(x_{1i}-\bar{x}_{*i})}{\sigma_{*1}\sigma_{*1}}$$

$$= r_{11} \quad \textit{(r is the Pearson correlation)} \tag{6}$$

Putting (6) *into* (5) *we get*

$$V = diag^{=0}\left(\begin{bmatrix} r_{11} & r_{12}\dots r_{1n} \\ r_{21} & r_{22}\dots r_{2n} \\ & \vdots \\ r_{m1} & r_{m2}\dots r_{mn} \end{bmatrix}\right) \cdot Z = \begin{bmatrix} 0 & r_{12}\dots r_{1n} \\ r_{21} & 0\dots r_{2n} \\ & \vdots \\ r_{m1} & r_{m2}\dots 0 \end{bmatrix} \cdot Z = \begin{bmatrix} \sum_{i=1}^{n}(z_i \times r_{1i}) - z_1 \times r_{11} \\ \sum_{i=1}^{n}(z_i \times r_{1i}) - z_2 \times r_{22} \\ \vdots \\ \sum_{i=1}^{n}(z_i \times r_{1i}) - z_n \times r_{nn} \end{bmatrix}$$

The elements of V *used for the decomposition (and subsequently the recovery) are computed by summing up the cross-correlation between the columns of* $\mathbf{X}$ *which concludes the proof.*

5 Incremental Scalable Sign Vector (ISSV)

In this section, we introduce a new incremental algorithm called ISSV to incrementally compute the maximizing sign vector in linear space. Then, we discuss the properties of the ISSV algorithm.

5.1 Incremental Weight Vector

Lemma 2 (Weight vectors are incremental) *Let* $Z^{(k)}$ *be* Z *at iteration* k*,* p *the positions of the last element flipped in* $Z^{(k)}$ *and let* v_i *be the* i*-th weight value in* V*. For any two consecutive iterations of sign vectors, the weight vectors are linearly dependent, i.e.,*

$$v_i^{(k+1)} = v_i^{(k)} - 2 \times (X_{i*} \cdot X_{p*}^T)$$

Proof 2 *By definition of the weight vector (cf.* (2)*) we have*

$$V^{(k)} = diag^{=0}(\mathbf{X} \cdot \mathbf{X}^T) \cdot Z^{(k)}$$
$$V^{(k+1)} = diag^{=0}(\mathbf{X} \cdot \mathbf{X}^T) \cdot Z^{(k+1)} \tag{7}$$

Let p *be the index of the element in* $Z^{(k)}$ *that has been flipped and let* U_p *be the unit vector with the same length as* $Z^{(k)}$ *where the* p*-th element is 1 and all other elements are 0. Using* U_p *we compute* $Z^{(k+1)}$ *as follows*

$$Z^{(k+1)} = Z^{(k)} - 2 \times U_p \tag{8}$$

Putting (8) into (7) we get

$$\begin{aligned} V^{(k+1)} &= diag^{=0}(\mathbf{X}\cdot\mathbf{X}^T)\cdot(Z^{(k)} - 2\times U_p) \\ &= diag^{=0}(\mathbf{X}\cdot\mathbf{X}^T)\cdot Z^{(k)} - 2\times diag^{=0}(\mathbf{X}\cdot\mathbf{X}^T)\cdot U \\ &= V^{(k)} - 2\times diag^{=0}(\mathbf{X}\cdot\mathbf{X}^T)\cdot U_p \end{aligned} \tag{9}$$

Let $col(\mathbf{X}, p)$ *return the p-th column of* $\mathbf{X}$*. Then, from (9) we get*

$$V^{(k+1)} = V^{(k)} - 2\times col(diag^{=0}(\mathbf{X}\cdot\mathbf{X}^T), p)$$

$$= V^{(k)} - 2\times \begin{bmatrix} X_{1*}\cdot X_{p*}^T \\ X_{2*}\cdot X_{p*}^T \\ \vdots \\ X_{n*}\cdot X_{p*}^T \end{bmatrix}$$

Thus, $\forall i \in [1,n]\setminus\{p\}$ *we have*

$$v_i^{(k+1)} = v_i^{(k)} - 2\times(X_{i*}\cdot X_{p*}^T) \tag{10}$$

Lemma 2 allows us to incrementally compute $V^{(k+1)}$ out of $V^{(k)}$ and subsequently to incrementally compute the maximizing sign vector. Unlike the iterative approach [18], the incremental approach does not require the construction of the intermediate vectors S and Z each of length n yielding faster computation. We compare the efficiency of both approaches in Section 6.

We propose an algorithm with linear space complexity to incrementally compute the maximizing sign vector Z according to the maximization problem introduced in (2). The basic idea is as follows. We begin with the sign vector $Z = [1,\ldots,1]^T$, change the sign of the element in Z that increases $Z^T\cdot V$ most, and incrementally compute the weight vector. The algorithm terminates when Z and V have the same pairwise sign.

Algorithm 2: ISSV($\mathbf{X}, n, m$)

Input : $n\times m$ matrix $\mathbf{X}$
Output: maximizing sign vector $Z\in[1,\text{-}1]^n$
1 $Z^T := [1,\ldots,1]$;
2 $V :=$ Compute initial weight vector ; ▷ `using` (3)
3 **repeat**
4 $\quad p := \{i \mid v_i = \min(v_j\in V)\,\&\, z_j\times v_j < 0\}$;
5 $\quad z_p := (\text{-}1)\times z_p$;
6 $\quad$ **foreach** $v_i \in V\setminus v_p$ **do**
7 $\quad\quad v_i := v_i - 2\times X_{i*}\cdot(X_{p*})^T$
8 **until** $p = 0$;
9 **return** $Z\in[1,\text{-}1]^n$;

Algorithm 2 implements the incremental strategy to compute the maximizing sign vector. We note that V is computed directly from $\mathbf{X}$ by reading the matrix row by row, one row at a time to compute the individual elements of V. We first compute

the initial weight vector according to (3). Then, we search for the index (p) of the element $v_i \in V$ with the largest absolute value such that v_i and $z_i \in Z$ have different signs, i.e., $z_i \times v_i < 0$. If such an element is found, the sign of z_i is flipped. A new vector V is incrementally computed out of the previous one, which is different from the vector in the previous iteration due to the sign change. The iteration terminates when the signs of all corresponding elements in V and Z are the same and thus, i.e., p is equal to 0. The vector Z in the final iteration is the maximizing sign vector that maximizes $Z^T \cdot V$.

Example 3 *To illustrate the computation of the sign vector using Algorithm 2, consider the same input matrix as the one introduced in our running example. We denote $Z^{(k)}$ as Z in the k-th iteration. First, Z is initialized with 1s, i.e., $Z^{(1)} = \{1,1,1,1,1\}^T$ and the initial weight vector is computed using* (3) *to get $V^{(1)} = \{-57,10,-46,9,-54\}^T$. All elements of $Z^{(1)}$ have a different sign from the corresponding elements in $V^{(1)}$ and among them the element in the 1st position has the highest absolute value. Using $p = 1$, the next weight vector is incrementally computed (using* (10)*) as follows*

$$
\begin{aligned}
v_1 &= -57 \\
v_2 &= 10 - 2 \times (\begin{bmatrix} 6 & 3 & 3 \end{bmatrix} \times \begin{bmatrix} -2 \\ 2 \\ 2 \end{bmatrix}) = 10 \\
v_3 &= -46 - 2 \times (\begin{bmatrix} 6 & 3 & 3 \end{bmatrix} \times \begin{bmatrix} -7 \\ 1 \\ -5 \end{bmatrix}) = 62 \\
v_4 &= 9 - 2 \times (\begin{bmatrix} 6 & 3 & 3 \end{bmatrix} \times \begin{bmatrix} -3 \\ 4 \\ -1 \end{bmatrix}) = 27 \\
v_5 &= -54 - 2 \times (\begin{bmatrix} 6 & 3 & 3 \end{bmatrix} \times \begin{bmatrix} 2 \\ -4 \\ 2 \end{bmatrix}) = -66
\end{aligned}
$$

i.e.,

$$
Z^{(2)} = \begin{bmatrix} -1 \\ 1 \\ 1 \\ 1 \\ 1 \end{bmatrix} \quad \textit{and} \quad V^{(2)} = \begin{bmatrix} -57 \\ 10 \\ 62 \\ 27 \\ -66 \end{bmatrix}.
$$

Only the 5th element in $Z^{(2)}$ has a different sign from the corresponding element in $V^{(2)}$, In the third iteration of the algorithm, we flip the sign of the element at position 5 in $Z^{(2)}$ and we use the new sign vector $Z^{(3)}$ to compute $V^{(3)}$, similarly to

the previous iteration, and get

$$Z^{(3)} = \begin{bmatrix} -1 \\ 1 \\ 1 \\ 1 \\ -1 \end{bmatrix} \text{ and } V^{(3)} = \begin{bmatrix} -69 \\ 26 \\ 118 \\ 75 \\ -66 \end{bmatrix}$$

Since all corresponding elements in $Z^{(3)}$ and $V^{(3)}$ have the same sign, the algorithm terminates and $Z^{(3)}$ is returned as the maximizing sign vector that maximizes $Z^T \cdot V$. Note that our technique computes the same sign vector as the one computed by the exhaustive search illustrated in Section 3.3.

Example 3 illustrates the main properties of the ISSV algorithm. In fact, the product $Z^T \cdot V$ is monotonically increasing at each iteration, i.e., $(Z^{(1)})^T \cdot V^{(1)} = -138$, $(Z^{(2)})^T \cdot V^{(2)} = 90$ and $(Z^{(3)})^T \cdot V^{(3)} = 354$. The algorithm terminates and computes the global optimum, i.e., 23.3.

The ISSV algorithm keeps in memory the sign vector V and one row of $\mathbf{X}^T$, each with $O(n)$ space complexity, where n is the number of rows in $\mathbf{X}$. To compute the individual elements $v_i = v_i - 2 \times X_{i*} \cdot (X_{p*})^T$ of the weight vector, $\mathbf{X}$ is read one row at a time. The result vector has length n, thus the total space complexity is $O(n)$. The total runtime complexity is $O(xn)$, where x is the number of flipped elements in the returned sign vector Z. The number of flipped elements depends on the number of negative rows in the input matrix and is on average less than third of the number of rows (n) (cf. Fig.10 in [18]).

5.2 ISSV Properties

In this section, we describe the main properties of the ISSV algorithm. Since ISSV uses the same definition of the weight vector as the SSV algorithm, the two algorithms share the same properties. More specifically, the computation of ISSV is monotonic, terminates and returns the correct result.

Let $Z^{(k)}$ and $V^{(k)}$ refer to, respectively, vectors V and Z in the k-th iteration of the ISSV algorithm. $v_i^{(k)}$ and $z_i^{(k)}$ denote, respectively, the i-th element of $V^{(k)}$ and $Z^{(k)}$. Lemma 3 shows that the computation of the maximizing sign vector in the ISSV algorithm is *strictly monotonic*, i.e., each iteration increases the value of $Z^T \cdot V$.

Lemma 3 (Monotonicity) *For any two consecutive iterations k and $k+1$ in the ISSV algorithm, the following holds:*

$$(Z^{(k+1)})^T \cdot V^{(k+1)} > (Z^{(k)})^T \cdot V^{(k)}.$$

Lemma 4 shows that ISSV does not flip a sign value more than once and thus terminates.

Lemma 4 (Termination) *Let $\mathbf{X}$ be an $n \times m$ matrix. ISSV($\mathbf{X}, n, m$) terminates and performs at most n iterations.*

Lemma 5 shows that our greedy approach computes the optimal solution.

Lemma 5 (Correctness) *The ISSV algorithm computes the maximizing sign vector for which the final product $Z^T \cdot V$ is the global maximum.*

The proofs of Lemma 3, 4 and 5 are described in detail in [18].

5.3 Flipping strategy

Lemma 6 (Local optimal choice) *The ISSV algorithm changes in each iteration the element of the sign vector Z that increases $Z^T \cdot V$ most.*

Proof 3 *We do a case analysis to prove that ISSV makes the local optimal choice.*

Case $z_i^{(k)} \times v_i^{(k)} < 0$*: The ISSV algorithm changes in each iteration the sign of an element* $z_i^{(k)}$ *that maximizes* $|z_i^{(k)} \times v_i^{(k)}|$*. Since* $diag^{=0}(\mathbf{X} \cdot \mathbf{X}^T)$ *is a symmetric matrix we have*

$$V^{(k)} = \begin{bmatrix} v_1 \\ v_2 \\ \vdots \\ v_{n-1} \\ v_n \end{bmatrix} = \underbrace{\begin{bmatrix} 0 & x_{12} & \dots & x_{1n} \\ x_{12} & 0 & \dots & x_{2n} \\ \vdots & \vdots & \ddots & \vdots \\ x_{1n-1} & x_{2n-1} & \dots & x_{n-1n} \\ x_{1n} & x_{2n} & \dots & 0 \end{bmatrix}}_{diag^{=0}(\mathbf{X} \cdot \mathbf{X}^T)} \cdot Z^{(k)}$$

Without loss of generality, we assume $z_1^{(k)} \times v_1^{(k)} < 0$*,* $z_n^{(k)} \times v_n^{(k)} < 0$ *such that* $|v_1^{(k)}| > |v_n^{(k)}|$*. Let* Z_1 *and* Z_n *be the sign vectors resulting from changing the sign of* z_1 *and* z_n *respectively. Then, we have*

$$(Z_1)^T \cdot V^{(k)} > (Z_n)^T \cdot V^{(k)}$$

$$(Z_1)^T \cdot (diag^{=0}(\mathbf{X} \cdot \mathbf{X}^T) \cdot Z^{(k)}) > (Z_n)^T \cdot (diag^{=0}(\mathbf{X} \cdot \mathbf{X}^T) \cdot Z^{(k)})$$

$$\sum_{i=2}^{n-1} x_{in} > \sum_{i=2}^{n-1} x_{1i} \tag{11}$$

Let's assume that we get a bigger benefit by changing the sign of z_n *instead of* z_1*. Then, we get*

$$(Z_1)^T \cdot V_1^{(k+1)} < (Z_n)^T \cdot V_n^{(k+1)}$$

$$(Z_1)^T \cdot (diag^{=0}(\mathbf{X} \cdot \mathbf{X}^T) \cdot Z_1) < (Z_n)^T \cdot (diag^{=0}(\mathbf{X} \cdot \mathbf{X}^T) \cdot Z_n)$$

$$\sum_{i=2}^{n-1} x_{in} < \sum_{i=2}^{n-1} x_{1i}$$

This contradicts Equation (11). Therefore, we get a bigger benefit by choosing the element that maximizes $|z_i^{(k)} \times v_i^{(k)}|$*, i.e.,* z_1.

Case $z_i^{(k)} \times v_i^{(k)} \geq 0$*: If instead we changed the sign of an element* $z_i^{(k)}$ *for which* $z_i^{(k)} \times v_i^{(k)} \geq 0$ *we get* $Z^{(k+1)} = Z^{(k)} + 2 \times U$ *(cf. Lemma 3), which implies* $(Z^{(k+1)})^T \cdot V^{(k+1)} \leq (Z^{(k)})^T \cdot V^{(k)}$*. Therefore,* $Z^T \cdot V$ *will not be increased.*

We now show that two alternative sign flipping strategies to compute the sign vector do not produce the global maximum.

Strategy 1: change at each iteration the sign of more than one element in Z. The maximization problem looks as follows:

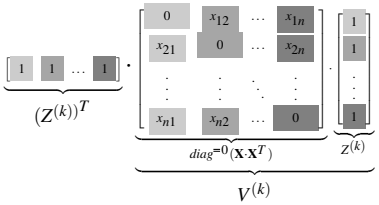

The result of the maximization is obtained first by multiplying the i-th element of $(Z^{(k)})^T$ with the i-th column of $diag^{=0}(\mathbf{X}\cdot\mathbf{X}^T)$, yielding a vector. Then, the i-th element of the resulting vector is multiplied again with the i-th element of $Z^{(k)}$. Thus, changing the sign of $z_i^{(k)}$ affects only the i^{th} column of $diag^{=0}(\mathbf{X}\cdot\mathbf{X}^T)$; all other columns are unaffected. Thus, the result of changing $z_i^{(k)}$ is independent from changing $z_j^{(k)}$ for $j \neq i$. Since we are maximizing over independent variables, the maximization of $(Z^{(k)})^T \cdot V^{(k)}$ is obtained by checking the result of changing one element in $Z^{(k)}$ at a time, and not if more than one element is changed.

Strategy 2: change at each iteration the sign of an element $z_i^{(k)}$ for which $z_i^{(k)} \times v_i^{(k)} > 0$. Following the same reasoning as in the proof of Lemma 3, we have $Z^{(k+1)} = Z^{(k)} + 2 \times U$, which implies that $(Z^{(k+1)})^T \cdot V^{(k+1)} < (Z^{(k)})^T \cdot V^{(k)}$. Therefore, this strategy is strictly monotonically decreasing and thus the global maximum will not be obtained.

6 Experimental Evaluation

This section evaluates in turn the performance of i) our CDRec (Recovery using CD) algorithm and ii) the ISSV algorithm that efficiently computes CD. For each experiment, we report the average result over five consecutive runs of the various algorithms.

6.1 Setup

6.1.1 Implementation

We compare CDRec against the state-of the-art missing-blocks recovery techniques: SSA [2], GROUSE [5], TeNMF [20], TKCM [30], STMVL [31], MRNN [32] and TRMF [33]. We rewrote all these algorithms in C++, except SSA and MRNN (we use the efficient original implementations). We use the same advanced linear algebra operations across all techniques, thanks to a modern library called Armadillo [28]. By using a common code infra-structure, we eliminate any source of disparities that would otherwise exist if each algorithm re-implemented common primitives. The source code and the datasets are available online[4].

All the following experiments were performed on a Linux machine with a 3.4 GHz Intel Core i7 and 16GB of RAM. The code was compiled with g++ 7.3.0 at the maximum optimization level.

6.1.2 Datasets

The following empirical evaluation was performed on real-world time series from different datasets containing time series of different correlation values (based on the Pearson correlation). Each tuple in the time series records a timestamp and the value of an observation. The values of the observations are stored as 4-byte floating numbers while the sign vectors are binary arrays. All the time series have been z-score normalized [15]. The *BAFU* dataset, kindly by the BundesAmt Für Umwelt (the Swiss Federal Office for the Environment) [12], contains water discharge time series collected from different Swiss rivers containing between 200k and 1.3 million values each, and cover the time period from 1974 to 2015. The *MeteoSwiss* dataset, kindly provided by the Swiss Federal Office of Meteorology and Climatology [21], contains weather time series recorded in different cities in Switzerland. Also, we use publicly available real-world time series: statistical quality control on *Baseball* time series [25], *Temperature* values of 703 climate stations in China collected from 1960 to 2012 [1] and *Gas* concentration batches that were gathered between 2007 and 2011 in a gas delivery platform facility situated at the ChemoSignals Laboratory at University of California San Diego [29,27]. For the gas dataset, we choose the longest batches to which we refer to as Gas6 and Gas10.

Table 1: Description of time series.

Name	Max_Length	# TS	granularity	r
BAFU TS	1.3M	12	30 min	[-0.03, 0.89]
MeteoSwiss TS	200k	7	10 min	[-0.12,0.9]
Baseball TS	2k	4	1 year	[-0.53, 0.49]
Temperature TS	19k	12	1 day	[0.78, 0.89]
Gas	3600	24	6hrs	[-0.75,0.78]

[4] `https://github.com/eXascaleInfolab/InCD_benchmark.git`

Table 1 describes the length, number, granularity and Pearson correlation coefficient (r)[5] of the time series we used in our experiments. The datasets we use here represent a broad range of applications. They contain time series which exhibit different levels of correlations which are representative of many aspects naturally present in real-world data.

6.2 Recovery Evaluation

In this section, we compare the accuracy and the efficiency of CDRec against the aforementioned techniques under different recovery scenarios.

6.2.1 Accuracy

In Table 2, we evaluate the accuracy of all the techniques using all datasets from Table 1. We set the length and the number of the time series respectively to their maximum per dataset. We first evaluate the case where the missing blcok appear in one time series. Then, we evaluate the case where the missing block appears in multiple time series. As accuracy measure we use the root mean square error (RMSE) between the original blocks and the recovered ones.

$$RMSE = \sqrt{\frac{1}{T}\sum_{t \in T}(x_t - \tilde{x}_t)^2}$$

where T is the set of missing values, x_t is the original value and $\tilde{x}_t$ is the recovered value.

On the left-hand side of Table 2, we set a missing block to appear arbitrarily in the middle of one of the series in the dataset. We then vary the size of the missing block from 20% to 80% (of the chosen series) and measure the recovery accuracy using RMSE. The results show that CDRec is on average 2.3x more accurate than the most accurate state-of-the-art algorithm, TRMF. Thanks to the weight vectors that embed the correlation across the input time series, CDRec is able to better leverage the similarity between time series and to accurately recover the missing blocks. The superiority of CDRec is more visible on datasets with high variations of correlation, e.g., Baseball and Gas datasets. We also observe that the error of CDRec does not always increase along with the size of the missing block in this experiment. In three datasets, Baseball Meteo, and Temperature the trend is the opposite. In these three datasets, larger missing blocks require a larger number of iterations which, in turn, yield better recovery.

On the right-hand side of Table 2, we vary the number of incomplete time series and we measure the recovery accuracy of all techniques, except TKCM and SSA which do not support this feature We create missing blocks with the size of 10% of the longest time series per dataset to appear completely at random in each time series. The results show that, similarly to the single incomplete case, CDRec outperforms its

[5] `https://en.wikipedia.org/wiki/Pearson_correlation_coefficient`

Table 2: Recovery accuracy on real-word datasets

	Method	varying % of miss. val. 20 %	40 %	60 %	80 %	varying # of incomplete TS 2	3	4
Baseball.	**CDRec**	**0.47**	**0.48**	**0.46**	**0.43**	**0.50**	**0.50**	0.92
	GROUSE	2.30	2.72	3.49	4.40	5.7	5.7	4.96
	MRNN	0.54	0.70	1.36	0.46	0.96	1.13	0.95
	SSA	0.47	0.54	0.50	0.51	-	-	-
	STMVL	1.05	1.08	1.06	1.05	1.10	0.97	1.01
	TeNMF	0.68	0.80	3.39	0.68	0.95	0.98	0.89
	TKCM	1.20	1.20	1.18	1.13	-	-	-
	TRMF	0.58	0.66	0.76	0.84	0.60	0.58	**0.77**
MeteoSwiss	**CDRec**	**0.05**	**0.04**	**0.03**	**0.05**	**0.04**	**0.09**	**0.15**
	GROUSE	5.35	4.99	4.25	4.32	5.90	4.86	4.80
	MRNN	0.31	0.42	0.62	0.51	0.35	0.42	0.48
	SSA	0.10	0.09	0.10	0.13	-	-	-
	STMVL	0.32	0.28	0.25	0.26	0.25	0.26	0.63
	TeNMF	0.07	0.08	0.08	0.31	0.09	0.13	0.83
	TKCM	0.13	0.14	0.27	0.40	-	-	-
	TRMF	0.05	0.05	0.04	0.15	0.04	0.23	0.28
Gas	**CDRec**	**0.08**	**0.1**	**0.23**	0.61	**0.56**	**0.58**	**0.55**
	GROUSE	0.31	0.27	1.01	0.98	0.52	2.87	2.70
	MRNN	0.37	0.77	0.68	**0.55**	0.79	0.74	0.95
	SSA	0.50	0.41	0.74	0.70	-	-	-
	STMVL	0.57	0.69	1.10	1.04	1.19	1.21	1.21
	TeNMF	0.62	0.61	0.81	0.91			
	TKCM	0.37	0.68	1.10	1.03	-	-	-
	TRMF	0.12	0.32	0.62	0.68	0.65	0.60	0.63
BAFU	**CDRec**	**0.07**	**0.08**	**0.15**	0.22	**0.20**	0.17	**0.16**
	GROUSE	0.62	0.48	0.60	0.54	0.47	0.42	0.38
	MRNN	0.42	0.46	0.48	0.49	0.43	0.43	0.39
	SSA	0.25	0.18	0.22	**0.20**	-	-	-
	STMVL	1.04	0.79	0.92	0.81	0.75	0.67	0.62
	TeNMF	0.09	0.10	0.29	0.39	0.18	**0.15**	0.17
	TKCM	0.42	0.48	0.47	0.52	-	-	-
	TRMF	0.17	0.14	0.42	0.47	0.24	0.20	0.18
Temp.	**CDRec**	**0.29**	**0.30**	**0.31**	**0.25**	0.28	**0.27**	**0.3**
	GROUSE	0.54	0.56	0.51	0.53	0.39	0.35	0.44
	MRNN	1.73	1.33	1.21	1.33	1.27	1.40	0.96
	SSA	0.31	0.34	0.32	0.37	-	-	-
	STMVL	0.45	0.45	0.4	0.42	0.32	0.30	0.37
	TeNMF	0.29	0.32	0.33	0.91	0.28	0.28	0.37
	TKCM	2.20	1.74	1.96	1.77	-	-	-
	TRMF	0.33	0.37	0.34	**0.33**	**0.27**	0.27	0.36

competitors in most datasets when multiple time series are incomplete. We observe also that in some datasets the error does not always increase along with the number of incomplete time series. As we stated earlier, the bigger the number of missing blocks, the more iterations the algorithms can perform to compute the recovery. More iterations mean further opportunities to refine the values with which the missing block was initialized.

We also evaluate the recovery accuracy when increasing the sequence length (n) and the sequence number (m). The results show similar trends as the ones depicted in

Table 2. In general, all techniques take advantage of longer and/or larger number of time series to improve the recovery.

In the experiment in Figure 1 we evaluate the impact of the position of the missing block on the recovery accuracy. We keep the length and number of time series to their maximum per dataset and we vary the position of the missing block starting after 5% of data. We set the size of the missing block to 10% of one time series and we choose the BAFU and Gas datasets which contain the longest and largest number of time series, respectively.

The results show two different trends. In the BAFU dataset (cf. Figure 1a), the accuracy of CDRec and TRMF is barely affected by the position of the missing block. For the remaining algorithms, however, the recovery drastically varies depending on the position. Most algorithms achieve their best recovery when the missing block occurs between 30% and 40% of data from the beginning. This part of the data contains a flat trend which poses no significant recovery challenge to most of the algorithms. In the Gas dataset (cf. Figure 1b), the accuracy of all algorithms deteriorates when the missing bock occurs between 40% and 50% from the beginning of the time series. The reason is that this part of the data contains lots of fluctuations which makes it harder for the algorithms to estimate the missing block. The results confirm that CDRec is still the best contender.

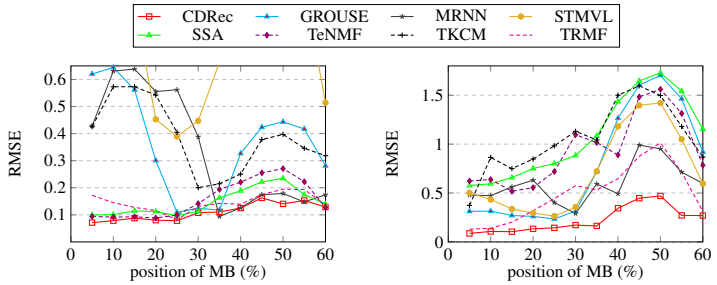

(a) BAFU dataset (b) Gas dataset.

Fig. 1: Accuracy comparison with moving the missing block (MB) position.

6.2.2 Efficiency

In this section, we compare the efficiency of CDRec by varying in turn the length of time series and second their number. We measure the elapsed runtime (wall clock) and we present it on a log scale since the results vary widely across algorithms.

In the experiment of Fig. 2, we set the number of time series to the maximum number per dataset, we vary their length between 200 and 2000 and measure the runtime (in ms) to recover a missing block of 100 observations (notice the log scale on the y axis). The results of this experiment show that CDRec is more efficient than its competitors with an average runtime equal to 5 ms to recover time series containing 2000 observations each. CDRec is on average 3x faster (3ms vs 10ms)

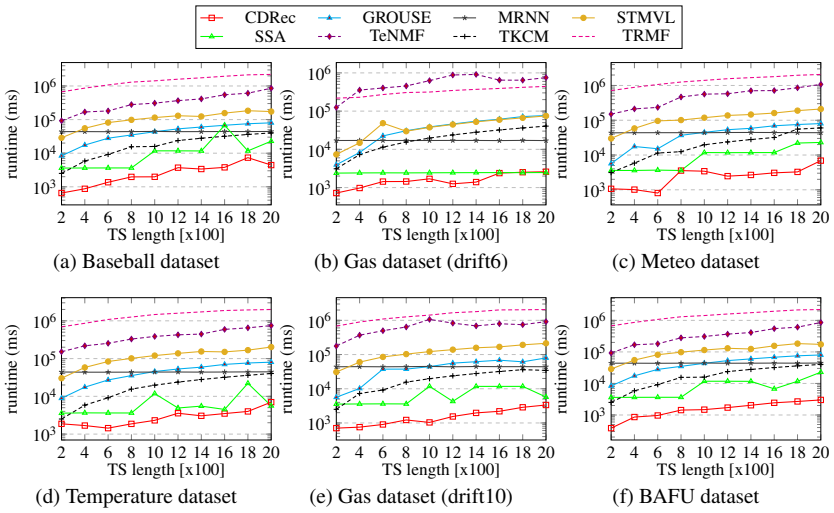

(a) Baseball dataset (b) Gas dataset (drift6) (c) Meteo dataset

(d) Temperature dataset (e) Gas dataset (drift10) (f) BAFU dataset

Fig. 2: Runtime varying TS length.

than the the fastest state of the art technique, SSA and two orders of magnitude faster than the most accurate state of the art technique, TRMF. The efficiency of CDRec is due to its fast incremental computation of the centroid values.

In the experiment of Fig. 3, we set the length of time series to $1k$, we vary their number from 4 to 12 and measure the runtime (in ms) to recover a missing block of 100 observations (notice the log scale on the y axis). We use the three datasets that contain up to 12 time series. The results of this experiment show that CDRec and SSA are the fastest solutions while TRMF and TeNMF are the slowest. Thanks to its effective entropy-based truncation procedure, the runtime of CDRec barely increases while increasing the number of time series used in the recovery.

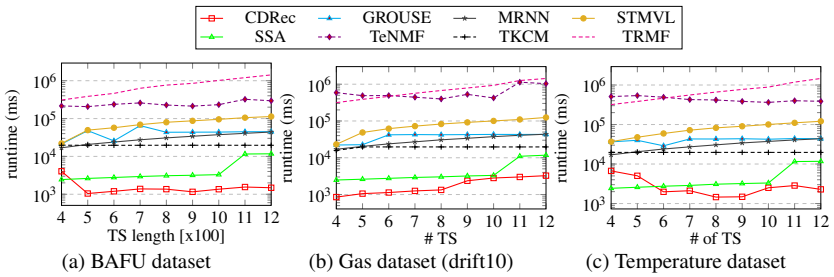

(a) BAFU dataset (b) Gas dataset (drift10) (c) Temperature dataset

Fig. 3: Runtime varying TS number.

6.2.3 Convergence

In the experiments in Fig. 4, we evaluate the convergence of the CDRec's recovery by measuring the number of iterations. In Fig. 4a, we set the number of time series to the maximum number per dataset and we vary the length of time series, while in Fig. 4b we set the length of time series to $1k$ and we vary the number of time series. The results of both experiments confirm that adding more observations and more time series helps CDRec reducing the number of iterations to perform the recovery until becoming constant at a specific number of observations ($1k$ values in the case of BAFU dataset), and at a specific number of time series also (8 time series in the same dataset). In Fig. 4c, we vary the missing percentage rate in time series and we measure the number of iterations. The result of this experiment confirms that CDRec algorithm converges in all datasets, i.e., the number of iterations does not exceed 100 for different missing rates in all datasets. It is worth noticing that the relative difference of Frobenius norm computed at each iteration of Algorithm 1 decreases monotonically until reaching the specified threshold.

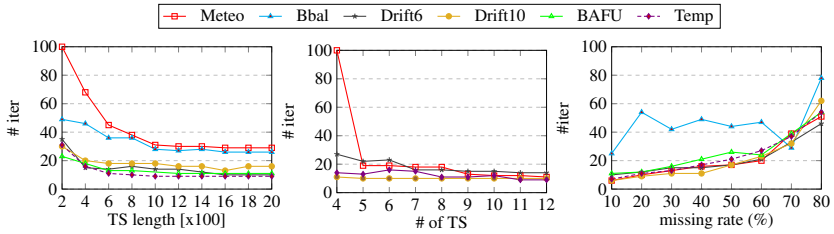

(a) Varying length of TS (b) varying # of TS (c) varying % of missing

Fig. 4: Recovery Convergence.

6.3 Matrix Decomposition

In this section, we evaluate different techniques to compare the CD technique. We refer to ISCD (our technique), SCD, and QCD as the Centroid Decomposition (CD) using respectively the ISSV, SSV, and QSV techniques (cf. Section 2.1).

6.3.1 Efficiency

In order to evaluate the efficiency of our technique, we choose the three datasets with the longest time series from Table 1. Fig. 5 evaluates the efficiency of our ISCD technique algorithm to decompose matrices of time series and compares it against SCD and QCD. In the experiments shown in Figs. 5a, 5b, 5c we set the number of time series to the max per dataset, we vary the length of time series to the max size per dataset and we report the runtime of the three algorithms. The results of this experiment show that for the largest BAFU dataset, ISCD is more than 3x faster than

SCD. The QCD algorithm runs out of memory for $n > 30k$, as it constructs an $n \times n$ correlation matrix. In the experiments shown in Figs. 5d, 5e, 5f we set the length of time series to $10k$ and $1k$ respectively, we vary their number between 10 and 100 (by splitting the time series into smaller segments) and we report the runtime of the three algorithms. The results of this experiment show that all the algorithms are linear with the number of time series. The results show also that in the BAFU dataset, ISCD is up to 9x faster than QCD (9min vs. 82min) and 7x faster than SCD (9min vs. 62min) while in the two other datasets, our ISCD is up to 12x faster than QCD (6 sec vs. 75 sec) and 6x faster than SCD (6 sec vs. 38 sec).

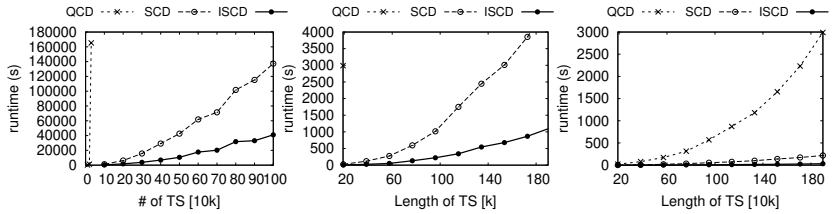

(a) varying # of rows on BAFU dataset. (b) varying # of rows on MeteoSwiss dataset. (c) [varying # of rows on Temp dataset.

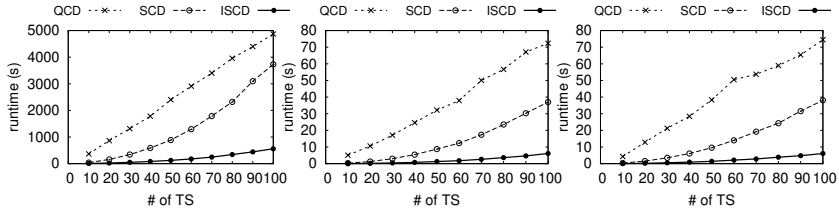

(d) [varying # of cols on BAFU datset. (e) [varying # of cols on MeteoSwiss dataset. (f) [varying # of cols on Temp dataset.

Fig. 5: Efficiency of different CD implementations.

6.3.2 Correctness

In this section, we evaluate the correctness of our technique using the Frobenius norm (cf. Section 4), FrobN, between the input matrix $\mathbf{X}$ and the matrix product $\mathbf{L} \cdot \mathbf{R}^T$ computed as a result of the decomposition. A correct CD decomposition returns $\mathbf{L}$ and $\mathbf{R}$ s.t. $\mathbf{X} = \mathbf{L} \cdot \mathbf{R}^T$ and subsequently $FrobN = 0$. In Table 3 we compare FrobN computed by ISCD against the one computed by the existing CD techniques. We vary the number of rows of a matrix containing the maximum number of time series (columns) per dataset, and compute FrobN for different n values. The results show that, unlike the QCD technique, the ISCD and SCD techniques return similar FrobN equal to zero for all datasets. Thus, both SCD and ISCD compute the correct CD decomposition while QCD yields an approximation of CD.

Table 3: Frobenius norm of different techniques.

FrobN / dataset	$n = 500$			$n = 1k$			$n = 2k$		
	SCD	ISCD	QCD	SCD	ISCD	QCD	SCD	ISCD	QSV
BAFU	6.7E-15	**6.5E-15**	33	2.3E-14	**2.4E-14**	52	4.1E-14	**3.9E-14**	58
MeteoS	5.6E-15	**5.6E-15**	18	7.9E-15	**7.9E-15**	27	1.9E-14	**1.9E-14**	44
Gas6	2.4E-14	**2.4E-14**	56	3.3E-14	**3.3E-14**	73	5.7E-14	**5.7E-14**	92
Baseball	6.4E-15	**6.5E-15**	14	1.8E-14	**1.8E-14**	23	-	-	-
Temp.	1.5E-14	**1.3E-14**	47	2.5E-14	**2.4E-14**	70	3.9E-14	**3.8E-14**	105
Gas10	2.1E-14	**2.1E-14**	66	3.8E-14	**4E-14**	78	4.6E-14	**4.6E-14**	90

7 Conclusion

In this paper, we first introduced the CDRec algorithm that uses the Centroid Decomposition technique to accurately recover missing blocks in time series with high variations in correlation. Then, we introduced the ISSV algorithm that efficiently computes the Centroid Decomposition in an incremental fashion, thus reducing the space complexity of the Centroid Decomposition from quadratic to linear. We conducted experiments on several real-world time series demonstrating that our technique outperforms the state of the art. The results show that CDRec is orders of magnitude faster than the most accurate algorithm while producing superior results in terms of recovery.

As future work, we plan to investigate the application of CDRec to perform continuous recovery of missing values in time series streams.

References

1. Administration, C.M.: Temperature TS , homepage: `https://www.hydrodaten.admin.ch/en` (Accessed: 2018-07-01)
2. Agarwal, A., Amjad, M.J., Shah, D., Shen, D.: Model agnostic time series analysis via matrix estimation. POMACS **2**(3), 40:1–40:39 (2018). DOI 10.1145/3287319. URL `https://doi.org/10.1145/3287319`
3. Agarwal, A., Amjad, M.J., Shah, D., Shen, D.: Time series analysis via matrix estimation. CoRR **abs/1802.09064** (2018). URL `http://arxiv.org/abs/1802.09064`
4. Alter, O., Brown, P.O., Botstein, D.: Singular value decomposition for genome-wide expression data processing and modeling. Proceedings of the National Academy of Sciences of the United States of America **97 18**, 10101–6 (2000)
5. Balzano, L., Chi, Y., Lu, Y.M.: Streaming pca and subspace tracking: The missing data case. Proceedings of the IEEE **106**(7) (2018)
6. Balzano, L., Nowak, R., Recht, B.: Online identification and tracking of subspaces from highly incomplete information. 2010 48th Annual Allerton Conference on Communication, Control, and Computing (Allerton) (2010). DOI 10.1109/allerton.2010.5706976
7. Bodik, P., Hong, W., Guestrin, C., Madden, S., Paskin, M., Thibaux, R.: Intel berkeley research lab dataset, homepage: `http://db.csail.mit.edu/labdata/labdata.html` (2004)
8. Cambronero, J., Feser, J.K., Smith, M.J., Madden, S.: Query optimization for dynamic imputation. PVLDB **10**(11), 1310–1321 (2017). DOI 10.14778/3137628.3137641. URL `http://www.vldb.org/pvldb/vol10/p1310-feser.pdf`
9. Chu, M.T., Funderlic, R.: The centroid decomposition: Relationships between discrete variational decompositions and svds. SIAM J. Matrix Analysis Applications **23**(4), 1025–1044 (2002). DOI 10.1137/S0895479800382555
10. D'agostino Sr, R.B., Russell, H.K.: Centroid Method. John Wiley and Sons, Ltd (2005). DOI 10.1002/0470011815.b2a13006

11. Dheeru, D., Karra Taniskidou, E.: UCI machine learning repository (2017). URL http://archive.ics.uci.edu/ml
12. for the Environment FOEN, F.O.: BAFU TS, homepage: https://www.meteoswiss.admin.ch/home.html?tab=alarm (Accessed: 2018-03-01)
13. Gold, M.S., Bentler, P.M.: Treatments of missing data: A monte carlo comparison of rbhdi, iterative stochastic regression imputation, and expectation-maximization. Structural Equation Modeling: A Multidisciplinary Journal **7**(3), 319–355 (2000). DOI 10.1207/S15328007SEM0703_1. URL https://doi.org/10.1207/S15328007SEM0703_1
14. Hening, D., Koonce, D.A.: Missing data imputation method comparison in ohio university student retention database. In: Proceedings of the 2014 International Conference on Industrial Engineering and Operations Management, Bali, Indonesia, January 7 – 9, 2014 (2014)
15. Jain, A., Nandakumar, K., Ross, A.: Score normalization in multimodal biometric systems. Pattern Recognition **38**(12), 2270–2285 (2005)
16. Jain, A.K., Nandakumar, K., Ross, A.: Score normalization in multimodal biometric systems. Pattern Recognition **38**(12), 2270–2285 (2005). DOI 10.1016/j.patcog.2005.01.012. URL https://doi.org/10.1016/j.patcog.2005.01.012
17. Khayati, M., Böhlen, M.H., Cudré-Mauroux, P.: Using lowly correlated time series to recover missing values in time series: A comparison between SVD and CD. In: Advances in Spatial and Temporal Databases - 14th International Symposium, SSTD 2015, Hong Kong, China, August 26-28, 2015. Proceedings, pp. 237–254 (2015). URL http://dx.doi.org/10.1007/978-3-319-22363-6_13
18. Khayati, M., Böhlen, M.H., Gamper, J.: Memory-efficient centroid decomposition for long time series. In: IEEE 30th International Conference on Data Engineering, Chicago, ICDE 2014, IL, USA, March 31 - April 4, 2014, pp. 100–111 (2014)
19. Lee, M., An, J., Lee, Y.: Missing-value imputation of continuous missing based on deep imputation network using correlations among multiple iot data streams in a smart space. IEICE Transactions **102-D**(2), 289–298 (2019). URL http://search.ieice.org/bin/summary.php?id=e102-d_2_289
20. Mei, J., de Castro, Y., Goude, Y., Hébrail, G.: Nonnegative matrix factorization for time series recovery from a few temporal aggregates. In: Proceedings of the 34th International Conference on Machine Learning, ICML 2017, Sydney, NSW, Australia, 6-11 August 2017, pp. 2382–2390 (2017)
21. of Meteorology, F.O., Climatology: MeteoSwiss TS, homepage: https://www.hydrodaten.admin.ch/en (Accessed: 2018-03-01)
22. Meyer, C.D.: Matrix Analysis and Applied Linear Algebra. SIAM (2000). DOI 10.1137/1.9780898719512. URL https://my.siam.org/Store/Product/viewproduct/?ProductId=971
23. Moritz, S., Sardá, A., Bartz-Beielstein, T., Zaefferer, M., Stork, J.: Comparison of different methods for univariate time series imputation in R. CoRR **abs/1510.03924** (2015). URL http://arxiv.org/abs/1510.03924
24. Ongie, G., Willett, R., Nowak, R.D., Balzano, L.: Algebraic variety models for high-rank matrix completion. In: Proceedings of the 34th International Conference on Machine Learning, ICML 2017, Sydney, NSW, Australia, 6-11 August 2017, pp. 2691–2700 (2017)
25. Rasp, J.: Statistical Quality Control, homepage: http://www.cma.gov.cn (Accessed: 2018-07-01)
26. Recht, B.: A simpler approach to matrix completion. Journal of Machine Learning Research **12**, 3413–3430 (2011)
27. Rodriguez-Lujan, I., Fonollosa, J., Vergara, A., Homer, M., Huerta, R.: On the calibration of sensor arrays for pattern recognition using the minimal number of experiments. Chemometrics and Intelligent Laboratory Systems **130**, 123 – 134 (2014). DOI https://doi.org/10.1016/j.chemolab.2013.10.012. URL http://www.sciencedirect.com/science/article/pii/S0169743913001937
28. Sanderson, C., Curtin, R.R.: A user-friendly hybrid sparse matrix class in C++. In: Mathematical Software - ICMS 2018 - 6th International Conference, South Bend, IN, USA, July 24-27, 2018, Proceedings, pp. 422–430 (2018). DOI 10.1007/978-3-319-96418-8_50. URL https://doi.org/10.1007/978-3-319-96418-8_50
29. Vergara, A., Vembu, S., Ayhan, T., Ryan, M.A., Homer, M.L., Huerta, R.: Chemical gas sensor drift compensation using classifier ensembles. Sensors and Actuators B: Chemical **166-167**, 320 – 329 (2012). DOI https://doi.org/10.1016/j.snb.2012.01.074. URL http://www.sciencedirect.com/science/article/pii/S0925400512002018

30. Wellenzohn, K., Böhlen, M.H., Dignös, A., Gamper, J., Mitterer, H.: Continuous imputation of missing values in streams of pattern-determining time series. In: Proceedings of the 20th International Conference on Extending Database Technology, EDBT 2017, Venice, Italy, March 21-24, 2017., pp. 330–341 (2017)
31. Yi, X., Zheng, Y., Zhang, J., Li, T.: ST-MVL: filling missing values in geo-sensory time series data. In: Proceedings of the Twenty-Fifth International Joint Conference on Artificial Intelligence, IJCAI 2016, New York, NY, USA, 9-15 July 2016, pp. 2704–2710 (2016)
32. Yoon, J., Zame, W.R., van der Schaar, M.: Estimating missing data in temporal data streams using multi-directional recurrent neural networks. IEEE Trans. Biomed. Engineering **66**(5), 1477–1490 (2019). DOI 10.1109/TBME.2018.2874712. URL https://doi.org/10.1109/TBME.2018.2874712
33. Yu, H., Rao, N., Dhillon, I.S.: Temporal regularized matrix factorization for high-dimensional time series prediction. In: Advances in Neural Information Processing Systems 29: Annual Conference on Neural Information Processing Systems 2016, December 5-10, 2016, Barcelona, Spain, pp. 847–855 (2016)
34. Zhang, S.: Nearest neighbor selection for iteratively knn imputation. J. Syst. Softw. **85**(11), 2541–2552 (2012). DOI 10.1016/j.jss.2012.05.073. URL http://dx.doi.org/10.1016/j.jss.2012.05.073
35. Zhu, X.: Comparison of four methods for handing missing data in longitudinal data analysis through a simulation study. Open Journal of Statistics **4**, 933–944 (2014). DOI http://dx.doi.org/10.4236/ojs.2014.411088